Journal of Materials Chemistry A

Understanding Extreme Fast Charge Limitations in Carbonate Mixtures

Journal:	*Journal of Materials Chemistry A*
Manuscript ID	TA-PER-10-2020-010166.R1
Article Type:	Paper
Date Submitted by the Author:	01-Jan-2021
Complete List of Authors:	Mallarapu, Anudeep; National Renewable Energy Laboratory Bharadwaj, Vivek; National Renewable Energy Laboratory, National Bioenergy Center Santhanagopalan, Shriram; National Renewable Energy Laboratory,

Understanding Extreme Fast Charge Limitations in Carbonate Mixtures

Anudeep Mallarapu,[1] Vivek Bharadwaj[1,2] and Shriram Santhanagopalan[2]

Center for Integrated Mobility Sciences, National Renewable Energy Laboratory,

Golden CO, 80401 USA

December 2020

Revised Manuscript Submitted

To

Journal of Materials Chemistry A

Contact Information:

Shriram Santhanagopalan
Center for Integrated Mobility Sciences
National Renewable Energy Laboratory
15013 Denver West Parkway | M/S 1633 | Golden, CO 80401
P 303-275-3944 | F 303-275-4415
https://www.nrel.gov/transportation/

---

[1] These authors contributed equally to this work.

[2] Corresponding Authors (Shriram.Santhanagopalan@nrel.gov, Vivek.Bharadwaj@nrel.gov)

Understanding Extreme Fast Charge Limitations in Carbonate Mixtures

Anudeep Mallarapu,[1] Vivek Bharadwaj[1,2] and Shriram Santhanagopalan[2]

Center for Integrated Mobility Sciences, National Renewable Energy Laboratory,

Golden CO, 80401 USA

Abstract

Charging large format lithium ion batteries within ten to fifteen minutes requires changes to the electrolyte composition in addition to modification of electrode and cell architectures. Several approaches to address this need have been proposed; but there is not a lot of clarity on understanding what factors limit the performance of existing electrolytes. This work takes a closer look at the solvated components of a mixture of $LiPF_6$ in ethylene carbonate (EC) and ethyl methyl carbonate (EMC) in the context of extreme fast charging and relates these findings to cell-level requirements. Molecular dynamics studies of the Gen-2 electrolyte compositions with increasing salt concentrations, have been performed to estimate transport properties like diffusivity, transference number and conductivity. Molecular-level differences in the structure of solvation shells under extreme $LiPF_6$ concentrations are probed here and some key aspects on solvent structure that help overcome barriers to Li^+ transport under extreme fast charge are discussed.

Keywords: Extreme Fast Charging, Solvation Shells, Transport Properties in Carbonate-based Mixtures

Understanding Extreme Fast Charge Limitations in Carbonate Mixtures

Anudeep Mallarapu,[1] Vivek Bharadwaj,[1,2] and Shriram Santhanagopalan[2]

Center for Integrated Mobility Sciences, National Renewable Energy Laboratory,

Golden CO, 80401 USA

1. Introduction

Lithium ion battery technology has improved significantly in terms of efficiency and energy density which has resulted in its increased adoption by automotive industry in production of battery electric vehicles (BEV). Limitations on charging times are still a major challenge for battery electric vehicles since conventional automobiles can be refueled much faster. Fast charging could increase BEV market penetration [1] by allowing consumers who do not have access to either residential or workplace charging to use it as their primary means of charging, in addition to alleviating range anxiety. Technical limitations associated with extreme fast charging including lithium plating, accelerated aging, poor thermal efficiencies, and electrolyte degradation have been extensively documented in recent literature.[2–5] Colclasure et al. [6] recently developed a continuum model to rank factors that limit fast charging performance at the electrode-level and identified poor electrolyte transport resulting in salt depletion within the anode and Li plating at the graphite/separator interface as the major contributor. The team recommended reducing tortuosity within the electrodes and/or operating at elevated temperatures; but pointed out that electrolyte limitations must be overcome to accomplish meaningful improvements to fast charging.

Several approaches have been proposed to overcome transport limitations in carbonate-based electrolytes for Li-ion cells. However, our understanding of factors that relate cell-level performance degradation under extreme fast charging to specific mechanisms of electrolyte degradation is still limited.[2] Liu et al.[7] also attributed poor fast charging performance to electrolyte mass transport limitations including

slow diffusion and low transference numbers that lead to incomplete utilization of active materials and recommended the use of Li-neutralized polyanions dissolved in polar aprotic solvents. The Li^+ conductivity in the presence of bulky polyanions has been discussed at length in the literature.[8,9] It has been challenging to maintain ionic conductivity while delivering adequate improvements to the transference numbers.[10]

A second strategy widely used to improve conductivity is the use of a low-viscosity co-solvent. Aliphatic esters (acetates and formates) have been widely used to improve electrolyte transport across a wide range of temperatures.[11,12] There are two limitations often associated with this approach: i) the reductive decomposition of the short chain esters at the anode surface interfere with the formation of a stable passivation layer resulting in shorter cycle life for these formulations.[9] ii) poor stability of these co-solvents against high voltage cathodes also limits the operating voltage window, resulting in lower energy densities. The use of nitrile-based solvents has been explored due to their high dielectric constants coupled with a low viscosity.[13–19] Poor solubility of lithium salts in aliphatic nitriles and limited voltage windows have been cited as reasons for why these molecules have not been widely adopted in battery electrolytes. More recently, the use of highly concentrated (> 4M) electrolytes has been suggested to improve reductive stability of nitrile-based solvents and enable fast charging. [20,21] A good overview of all these strategies is summarized in a recent review by Logan and Dahn.[22]

To overcome impedance build-up with ester-based solvents and balance conductivity against electrochemical stability, Smart et al. investigated the properties of a series of quaternary mixtures of carbonates consisting of EC/DEC/DMC/EMC. The authors also documented the importance of localized interactions, in addition to bulk properties in influencing electrolyte performance.[23] Other groups have also documented via experiments, the importance of considering localized phenomena as opposed to screening electrolytes based on bulk properties such as dielectric constants.[24] To date, a mixture of

cyclic carbonates, such as ethylene carbonate (EC) or propylene carbonate (PC), and linear carbonates such as ethyl methyl carbonate (EMC), dimethyl carbonate (DMC) or diethyl carbonate (DEC) has been the most successful electrolyte formulation that meets most of the requirements for use in lithium ion batteries.[25] Experimentally measured values for transport properties of Li^+ in these electrolytes as a function of salt concentration as well as temperature has been widely reported. [26,27] Extensive modeling efforts have also been undertaken on these systems. [28–32] Molecular modeling of electrolytes provides a method to screen potential candidates and optimize electrolytes under numerous conflicting requirements. Quantum chemistry calculations and classical molecular dynamics calculations have been used to gain significant insights into solvation structures and transport properties for several solvents at various concentrations. [33,34] The composition of Li^+ solvation sheath plays a very important role in solid-electrolyte interface (SEI) chemistry and performance of the battery.[35] Molecular dynamics simulations have been used to study how solvent composition affects the structure and dynamics of lithium solvation shell in non-aqueous electrolytes.[36] Accurate force fields have been mandated as a pre-requisite for making good prediction of electrolyte properties.[37] Several approaches, including reactive force fields have been proposed.[31] Both non-polarizable and polarizable force-field have also been used in molecular dynamics simulations. Even though non-polarizable force-fields have been successful in reproducing structural properties of electrolytes, transport properties like diffusivity are often underpredicted.[38] Nonetheless, MD simulations provide crucial molecular-level insight into the solvation structure of various electrolyte compositions and play a crucial role in enabling the rational design of novel performance advantaged electrolyte molecules.

In this study, we use classical molecular dynamics simulations to study the dependence of transport properties and changes in structural properties of the electrolyte with salt concentration. We use a 3:7 wt.% EC-EMC solvent, which is consistent with the solvent formulation for the Gen-2 electrolyte, at four

different $LiPF_6$ concentrations. Specifically, we examine the structure and composition of the solvation sheath around lithium ions to interpret their implications for transport at the macroscale and identify electrolyte design principles that will help overcome these limitations and enable extreme fast charging. To this end, we compute the self-diffusivities from MD calculations and use these as input to generate effective Fickian diffusion coefficients, transference numbers and Li^+ conductivities as a function of salt concentration. Next, we employ target values for these properties prescribed by continuum-scale simulations to analyze what features on the solvation structure and composition of the electrolyte will enable the design of candidate solvents or additives suitable for extreme fast charging.

2. Computational Methodology

2.1. QM calculations for point charges

For the accurate representation of charge distribution amongst the solvent molecules (EC and EMC) and PF_6^-, their structures were geometry optimized at the B3LYP/6-311++g(d,p) [39,40] level using the Gaussian16 package. [41] This was chosen as Zhang et. al recently demonstrated that this method provides reliable point charges for electrolyte molecules. [42] The point charges were then derived using restricted electrostatic potential (RESP) method. [43] Uniform scaling of the point charges was not adopted since the focus of this manuscript was to reproduce experimental trends and not specific values.

2.2. Classical Molecular Dynamics

Molecular dynamics simulations on Li^+-PF_6^--EC-EMC systems were conducted for 4 systems with increasing molarities of Li^+-PF_6^- (Table 1). The antechamber [44] tool was employed to generate parameter files for EC and EMC molecules using the RESP derived point charges along with the geometric (bonds, angles, dihedrals) and non-bonded parameters from the generalized amber forcefield (GAFF). [45] The atom types and geometric parameters for PF_6^- were obtained from Chaumont et al. [46] The Amber format prep files listing RESP derived point charges for EC, EMC and PF_6^- are included in

Section S2 of the supplementary information. The parameters for Li^+ ion were obtained from Joung et al. [47] The GAFF forcefield with RESP derived point charges has been demonstrated to accurately reproduce the transport properties of electrolytes in addition to ionic liquid and other solvated condensed phase systems. [42,48–51] While the topology and coordinate files were generated using AmberTools, the open-source package LAMMPS was used as the molecular dynamics engine. The conversion of Amber format files to LAMMPS format was done using the Intermol package.[52] Packmol was used to generate initial solvated configurations for the 4 systems.[53] The simulation protocol for the solvated systems involved initial equilibration for 1 ns in the isobaric-isothermal ensemble at 1 bar and 298K. The computed densities were observed to plateau to within 5% of the experimental values for systems with similar molarities. This was followed by a production run for 25 ns in the canonical (NVT) ensemble. The particle-particle particle-mesh (pppm) technique [54] with a long-range cut off of 12 Å was considered for non-bonded interactions. All simulations were conducted with a time-step of 1 fs and considered periodic boundaries. Velocities and coordinates for the MD trajectories were saved every 0.1 ps. The python LAMMPS analysis tool (pyLAT) was used for analysis of trajectories for transport properties (diffusivities, conductivities, ion-pair lifetimes) and characterizing the solvated structures (radial distribution functions, coordination numbers).[55] The volmap tool in VMD was used for visual analysis of the trajectories.[56]

Table 1. Composition and properties of electrolyte systems considered in this study

System	Number of molecules				Density (MD)	$LiPF_6$ Molarity
	EC	EMC	$[Li]^+$	$[PF_6]^-$	(g/cc)	(M)
A	716	1422	20	20	1.156	0.108
B	716	1422	100	100	1.196	0.528
C	716	1422	200	200	1.236	1.023
D	716	1422	400	400	1.310	1.926

2.3. Binding Energy Calculations

The software package Gaussian16 [57] was used to perform quantum chemistry calculations to extract binding of lithium in gas phase with EC and EMC. Both cis and trans configurations of EMC are considered with lithium ion positioned both towards carbonyl oxygen and away from it giving a total of four configurations. For EC, binding energy is calculated only with the ion at the carbonyl oxygen since using the initial position closer to non-carbonyl oxygens resulted in lithium ion moving towards the carbonyl oxygen after static relaxation. All the binding energy calculations were performed at M062x level of theory [58] and the 6-311G(2d,d,p) basis set in the gas phase.[59]

3. Results and Discussion

Calculation of solvation structures as a function of solvent composition [25,60] including the effect of additives [61] and salt concentrations [17] have been reported before. Experimental ranking of the solvating power of various electrolyte solvents for lithium batteries has also been attempted.[24] Mapping of device level requirements to molecular structures is a crucial gap currently not addressed in the literature, in considering choice of solvents for fast charging. Continuum-scale simulations have stipulated[6] twice the conductivity against the baseline values for the Gen-2 electrolyte, three-to-four times the diffusivity, and a transference number of 0.5–0.6 as requirements for enabling charge rates of 4C through 6C. Whereas individual solvents can meet a subset of these requirements under specific operating conditions, there are constraints specific to fast charge such as higher frequency of solvation, longer solvation times and the need for maintaining conductivities at twice the average salt concentration (1.2 M) to account for sharp local gradients within the electrodes. We start by examining transport properties of the electrolytes computed using classical molecular dynamics and compare these against the effective properties in the solution. Next, we attempt to understand these trends in light of the solvation shell structures and energies for the various species in the electrolyte to solvate charge carriers at different concentrations. We conclude with a discussion of features identified on the solvation structure that will

likely help improve transport properties for extreme fast charge and how to tailor the solvent molecules towards these goals.

3.1. Binding Energy Calculations

Considering the flexible structure of the EMC electrolyte and the multiple possible interaction sites for Li^+, we conducted gas phase biding energy calculations to evaluate four possible configurations of Li^+ interacting with EMC (Figure 1). Our gas-phase binding energy calculations indicate that the 4 possible Li^+-EMC binding configurations are within a 1 kcal/mol of each other and may not be considered to be particularly preferential. However, as discussed later, from our volumetric probability density maps (Section 3.5, Figure 6) we do observe significantly more Li^+ interaction with the carbonyl oxygen sites which is statistically more representative of Li^+-EMC behavior in a solvated system.

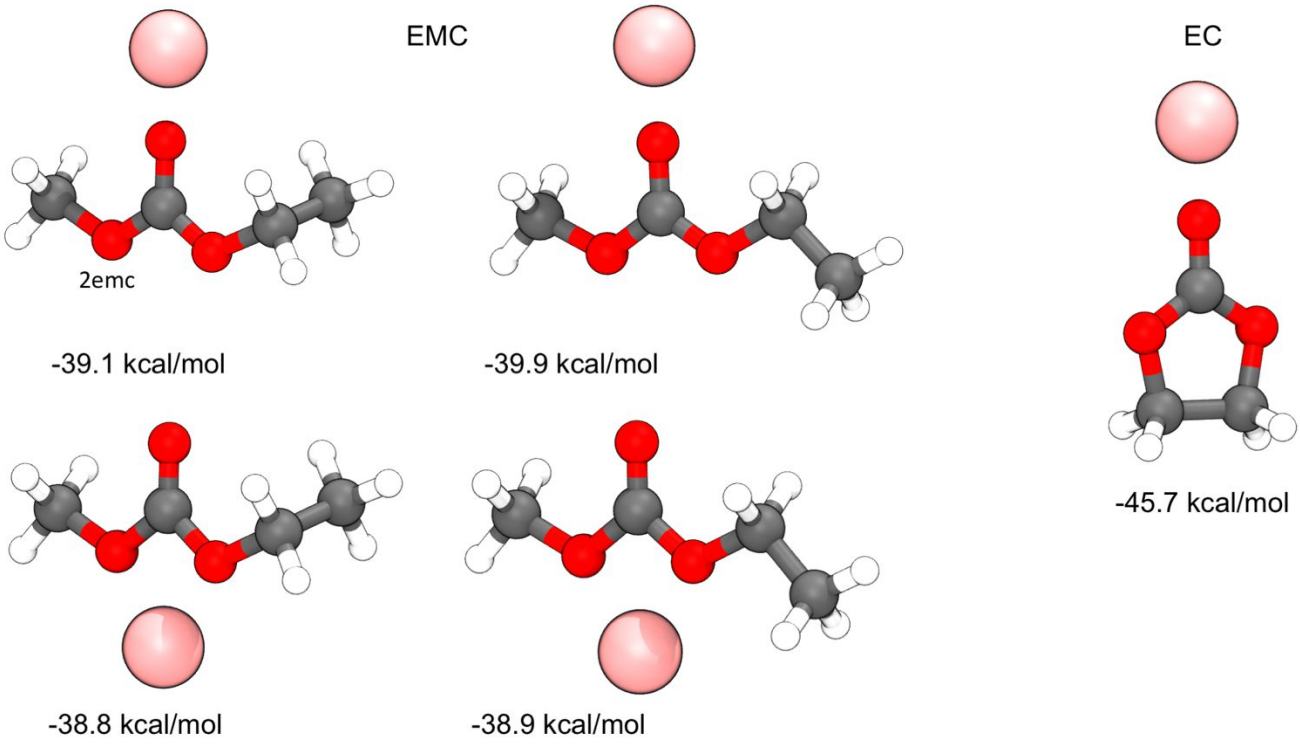

Figure 1. Lithium ion interactions with EC and EMC molecules. The gas-phase binding energy for each configuration is reported in kcal/mol. Lithium ions interacting with the EMC molecule do not show a preference for a particular oxygen site over others in the gas phase calculations, unlike the Li^+-EC interactions which are dominated by the carbonyl group. Changes to this behavior in a solvated system are discussed in subsequent sections.

This is likely due to the freely rotatable bonds in EMC. In contrast, although EC has two ring oxygens in addition to the carbonyl oxygen, Li^+ was observed to only bind with the carbonyl oxygen. It is also noted that the Li^+-EC binding energy is ~6 kcal/mol greater than that for Li^+-EMC.

3.2. Classical Molecular Dynamics

The gas-phase QM calculations provide us with only limited insight into the Li^+ interactions with EC and EMC with binding energies and only account for the interaction between the one ion and electrolyte molecule. The conditions inside a Li-ion battery are far different with a much more crowded environment accompanied by competitive interactions with neighboring electrolytes, both identical and otherwise, and other ions. In order to explore the Li^+-electrolyte behavior in this solvated system, we set-up molecular dynamics systems with statistically significant number of electrolyte molecules and salt concentrations relevant to experimental systems. The analysis of the MD simulations yields transport properties and molecular-level insight into the changes in solvation structure with increasing salt concentration. The MD simulations conducted using LAMMPS were analyzed using PyLAT. [55]

3.3 Diffusivity Calculations

The self-Diffusivity (D_{ii}) of each species *i* can be computed from molecular dynamics trajectories using the mean-squared displacement (MSD) as follows:

$$D_{ii} = \frac{1}{6} \lim_{t \to \infty} \frac{d}{dt} [r(t) - r(0)]^2 \quad (1)$$

where *r(t)* is the position of molecule/ion varying with time and *r(0)* is the initial position. Self-diffusivity of each component in the mixture decreases with an increase in salt concentration. The solvated Li^+ ion has the lowest diffusivity owing to the solvation shell around the ion affecting its mobility.

As discussed earlier, local composition of the electrolyte within each electrode can vary significantly under fast charge conditions, frequently resulting in salt concentrations upwards of 2M. The interactions

across different species present within the electrolyte are particularly important when considering such concentrated electrolytes. The cross-diffusion terms of the Stefan-Maxwell diffusivity (D_{ij}) are used to capture these interactions. (See supplementary information: S1) We use the generalized Darken formulation adopted by Kim and Srinivasan [62] to compute these terms from the self-diffusivity of the individual species:

$$D_{ij} = \frac{x_i}{x_i + x_j} D_{jj} + \frac{x_j}{x_i + x_j} D_{ii} \tag{2}$$

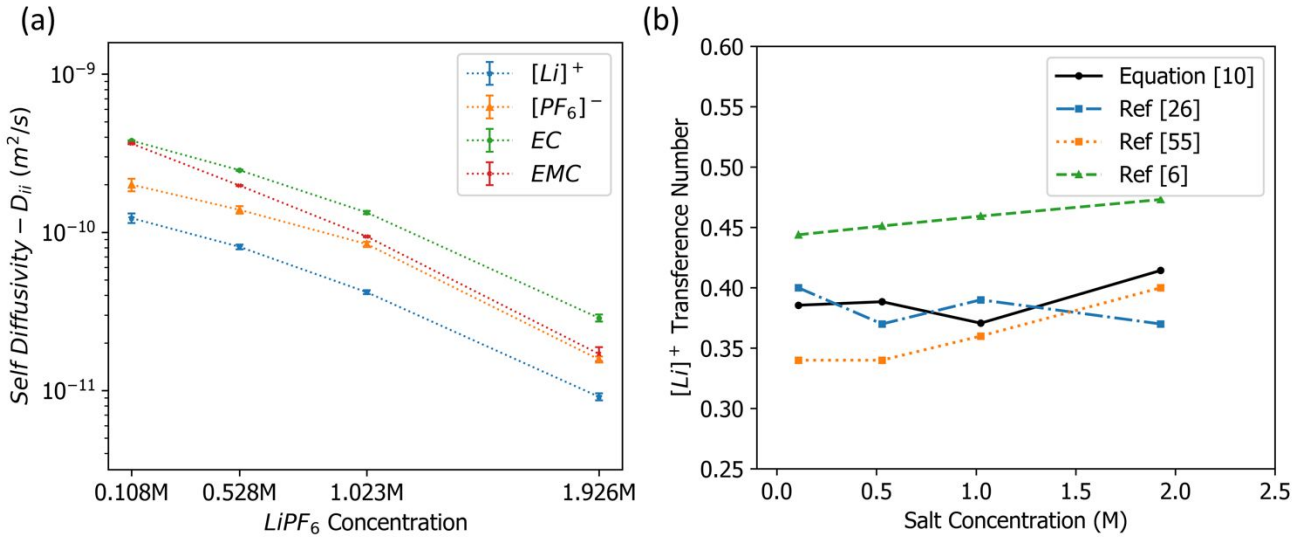

Figure 2. (a) Self-diffusivity of the components in the electrolyte decreases with increasing salt concentrations due to an increase in the bulk viscosity of the electrolyte. The error bars represent ± one standard deviation and are of the same magnitude as the size of the markers. (b) Transference numbers calculated from our MD results compare well against experimentally measured values from the literature.

The effective binary diffusivities for Li^+ and PF_6^- with respect to the solvent are then computed using: [63]

$$D_{+,0} = \frac{(1 - x_{Li^+})}{\frac{x_{EC}}{D_{Li^+,EC}} + \frac{x_{EMC}}{D_{Li^+,EMC}}} \tag{3}$$

$$D_{-,0} = \frac{(1 - x_{PF_6^-})}{\frac{x_{EC}}{D_{PF_6^-,EC}} + \frac{x_{EMC}}{D_{PF_6^-,EMC}}} \tag{4}$$

These effective binary diffusivities are related to the thermodynamic diffusion co-efficient by the following expression: [64]

$$\mathrm{D} = \frac{(z_+ - z_-)D_{+,0}D_{-,0}}{z_+ D_{+,0} - z_- D_{-,0}} \tag{5}$$

A thermodynamic correction factor is often used to correct for structural interference of the solvent molecules with transport. In here, we use the experimental data for the Gen-2 electrolyte from Stewart and Newman:[27]

$$1 + \frac{d\ln \gamma_{\pm}}{d\ln m} = c_0 \overline{V}_0 \left\{ 1 + c\left[\frac{-1.0178}{2(1 + 0.9831\sqrt{c})} \left(\frac{1}{\sqrt{c}} - \frac{0.9831}{1 + 0.9831\sqrt{c}} \right) + 1.5842 \right] \right\} \tag{6}$$

Equation (6) is an empirical expression fit to experimental data; hence, the choice of units for the different variables needs close attention. c_0 is the concentration of the solvents in mol/l computed using $c_0 = \sum_k \rho_{0,k}/\mathrm{M}_{0,k}$ where $\rho_{0,k}$ are the densities of the pure solvents and $\mathrm{M}_{0,k}$are their respective molecular

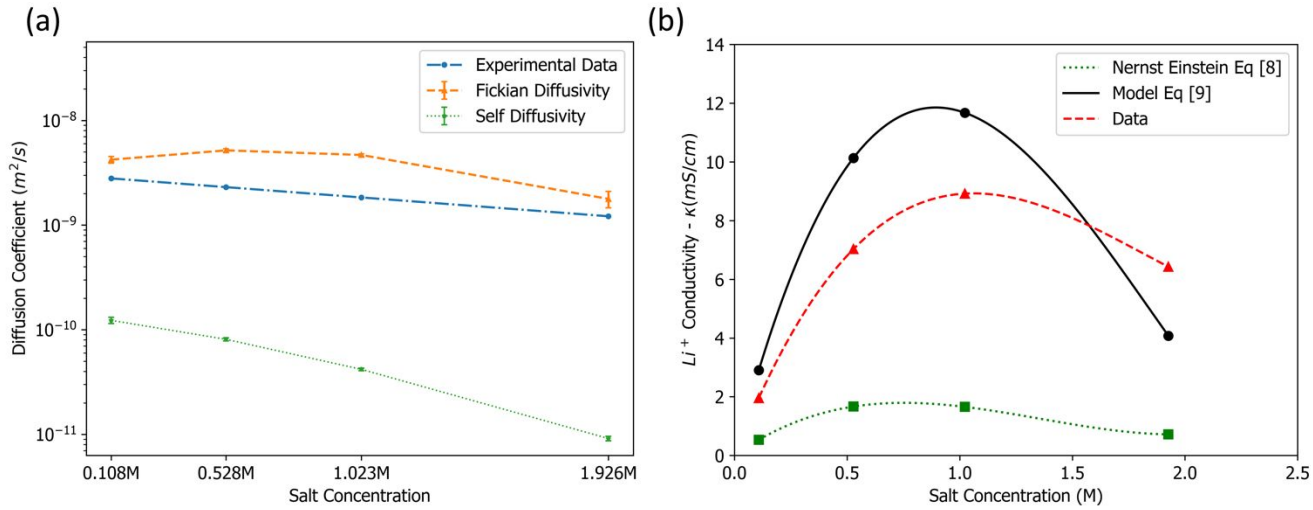

Figure 3. Comparison of effective transport properties against experimental data: (a) self-diffusivity and Fickian diffusivity for Li^+ (error bars represent $\pm$ one standard deviation) in the Gen-2 electrolyte against experimental values[6]: the thermodynamic correction factor (See equation 6) is a major contributor to bringing the Fickian diffusivities closer to experimentally measured values. (b) Conductivity values

computed using the Onsager-Stefan-Maxwell formulation matches experimentally reported values for Li^+ conductivity in the Gen-2 electrolyte.

weights. $\overline{V}_0$ is the partial molar volume of the solvent. The Fickian diffusion coefficients often used in continuum-scale simulations are then computed as follows:

$$D_e = \mathrm{D}\frac{c_T}{c_0}\left(1 + \frac{d\ln \gamma_{\pm}}{d\ln m}\right) \tag{7}$$

A comparison of the self-diffusion co-efficient for lithium against the calculated (equation 7) and experimentally measured [6] effective Fickian-diffusivity as a function of salt concentration is shown on Figure 3. Considering that experimentally measured diffusion coefficients are only accurate to an order of magnitude, the MD simulations predict the Fickian diffusivities reasonably well.

3.4 Ionic Conductivity and Transference Number

Ionic conductivity (κ) is usually estimated from self-diffusivities using the Nernst-Einstein relationship:[61-62]

$$\kappa = \frac{e^2}{k_B T V}\sum_i N_i q_i^2 D_i \tag{8}$$

However, the Onsager-Stefan-Maxwell formulation accounts for the interaction between the charge carriers as well as those with the solvent:[64]

$$\frac{1}{\kappa} = \frac{-RT}{F^2 z_+ z_- c_T}\left[\frac{1}{D_{+,-}} + \frac{c_0 t_-^0}{c_{Li^+} D_{-,0}}\right] \tag{9}$$

where t_-^0 is computed from the Li^+ transference number (t_+^0) using the following expression:

$$t_+^0 = 1 - t_-^0 = \frac{z_+ D_{+,0}}{z_+ D_{+,0} - z_- D_{-,0}} \tag{10}$$

From the target values for transport properties specified at the beginning of Section 3, and results shown in Figure 2b we gather that a 25 to 50% enhancement to the values of t_+^0 is required to achieve the fast

charge goals. At very low salt concentrations, the ionic conductivity is limited by the availability of charge carriers. With increasing salt concentrations, κ increases due to adequate number of ions being available to transport charge. But as the salt concentration increases further, drop in pairwise diffusivities due to strong interaction of the solvent molecules with neighboring species limits the ionic conductivity. This latter result correlates well with the experimentally observed increase in viscosity of the electrolyte at higher salt concentrations.

In equation (7), there are two contributions to the Fickian diffusivity: the first term is the thermodynamic diffusivity D, which is computed directly from the self-diffusivity values for the different species obtained from MD simulations. This term accounts for the interaction of Li^+ with the solvent molecules under ideal conditions (i.e., where there are no limitations imposed by say, steric hinderance of the adjoining entities, to the interaction between the charge carrier and the solvent). The correction factor introduced in equation (6) accounts for these interactions and thus makes the calculated values relevant to experimental results. As seen from Figure 1, the role of steric interactions is quite significant in these systems, and increasingly so at higher salt concentrations.

3.5 Solvation Structure

Coordination numbers obtained from molecular dynamics simulations (Table 2) give us a picture of solvation shell composition. The location of the solvent molecules (both EC and EMC) closer to the Li^+ compared to the location of the PF_6^- ions confirms good solvation using these molecules and affirms the choice of PF_6^- as a good candidate for the counterion. Even though binding energy calculations show that EC has a higher preference for binding with Li^+, molecular dynamics results indicate that EMC has a higher coordination number with the lithium ion in the first solvation shell. A more detailed understanding of the coordination numbers can be obtained from the radial distribution functions (RDF) shown in Figure 4, which are a plot of likelihood of occurrence of a specific pair-wise ion-solvent interaction as a function

of distance from the center of the ion. The RDF for each solvent molecule is plotted with respect to Li^+ to gain preliminary insights into the structure of solvation shell around Li^+. The RDF plots of EC and EMC molecules with respect to lithium ion also indicate a preference for EMC binding with Li^+. This is likely an artifact of having twice the number of EMC molecules in our system and binding energies changing in the solution phase as opposed to the gas phase.

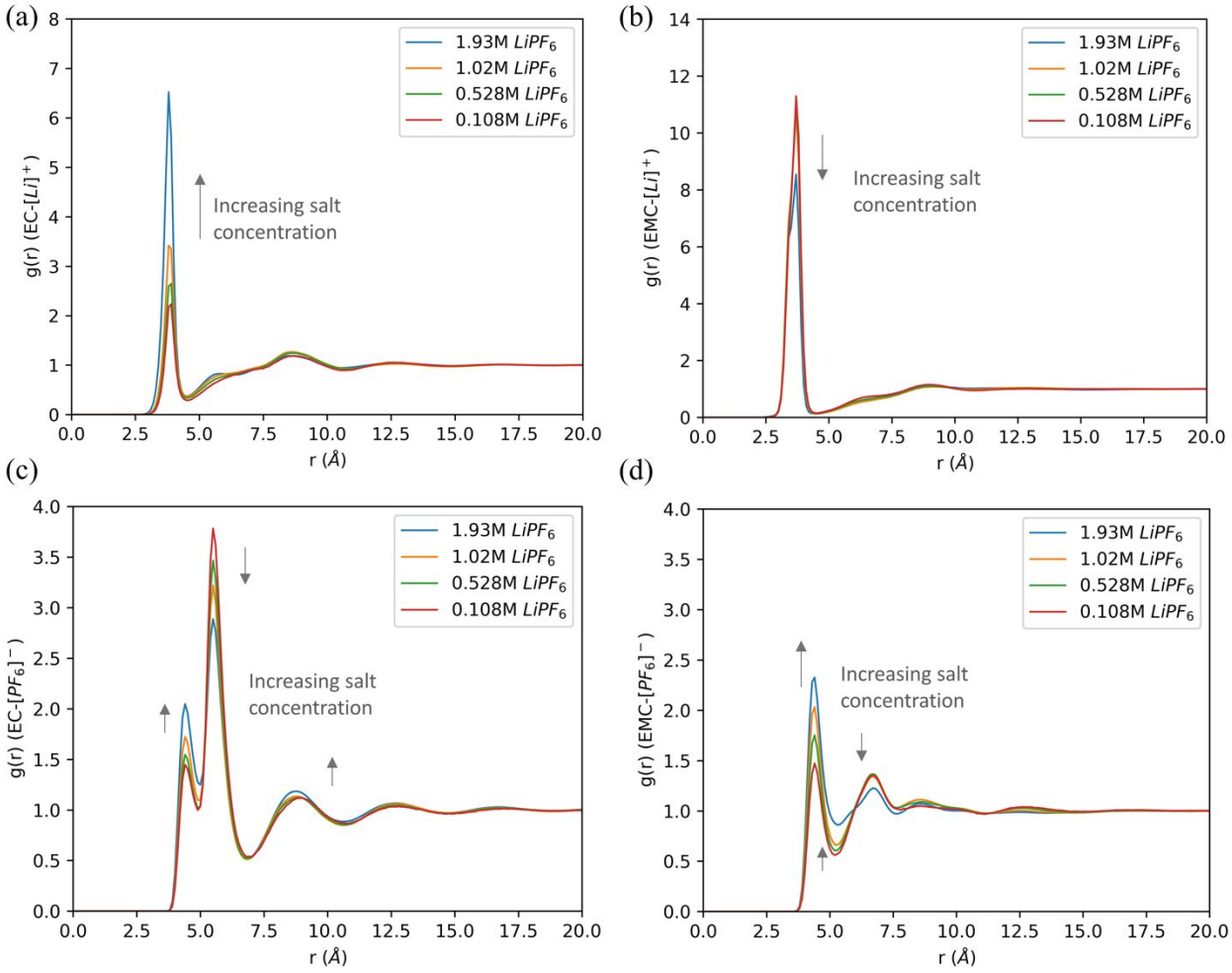

Figure 4. Radial distribution functions of solvent molecules EC, EMC with respect to Li^+ (a, b respectively) and PF_6^- (c, d respectively).

Our simulations indicate a consistent decrease in Li-EMC interactions that is accompanied by a consistent increase in Li-EC interactions with increasing salt concentrations. This observation is also consistently reflected in the coordination numbers in Table 2.

Table 2. Coordination numbers indicate a consistent decrease in Li-EMC interactions that is accompanied by a consistent increase in Li-EC interactions with increasing salt concentrations

System	PF_6^- around Li^+	EC around Li^+	EMC around Li^+	EC around PF_6^-	EMC around PF_6^-
Distance from center	7.5 Å	4.5 Å	4.5 Å	4.9 – 5.0 Å	5.2 – 5.3 Å
A (0.108M)	0.2457	0.5266	4.7303	0.6609	1.5022
B (0.528M)	0.6789	0.6092	4.5891	0.6812	1.6998
C (1.023M)	1.1722	0.7408	4.3454	0.7282	1.9866
D (1.926M)	2.1508	1.1629	3.2882	0.9039	2.2408

From RDF plots of PF_6^- - Li^+ (Figure 4), we see that at lower concentrations the peak at the smallest distance is lower than the peaks at larger distances. This is again, a result of high degree of dissociation of $LiPF_6$ salt. As the concentration increases, the peak closest to the center of the ion increases and the other peaks reduce due to a smaller fraction of the salt dissociating. This is indicative of the fact that the dissociation of Li^+-PF_6^- is hindered at larger salt concentrations and might be the primary reason for the observed drop in Li^+ transport parameters in Figure 2.

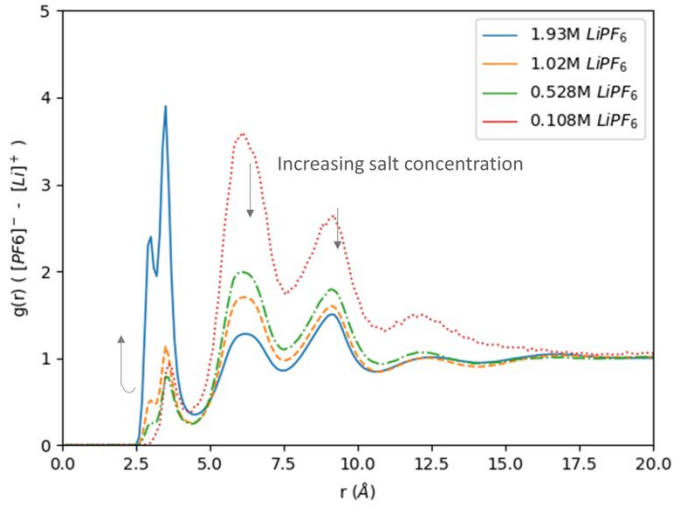

Figure 5. Radial distribution functions of PF_6^- with respect to Li^+ at increasing salt concentrations (0.108 M in red, 0.528 M in green, 1.02 M in orange and 1.93 M in blue). Sharp peaks at ~3 Å indicate greater association of Li+ and PF_6^- at high salt-concentrations.

We also infer that the formulation of an ideal electrolyte composition with the optimum Li-ion transport performance will ultimately be dictated by the solvation structure at the molecular level. These results are in agreement with the observation from Table 2 that the sum of the coordination numbers for Li^+-EC and Li^+-EMC decreases with salt concentration while that for Li^+-PF_6^- increases.

Molecular simulations offer the unique opportunity to explore the impact of molecular structure on the solvation and ordering in condensed phase systems. The volumetric probability density maps shown in Figure 6 depict the probability of finding a given molecular moiety around another molecular moiety in a 3-D space. For the EC molecule, the volumetric probability density maps indicate clearly demarcated regions for PF_6^- and Li^+ interactions. The carbonyl oxygen on EC being negatively charged offers the only favorable site for Li^+ interaction while the -CH_2 groups on the ring structure of EC being diametrically opposite provide the only sites of interaction for PF_6^-.

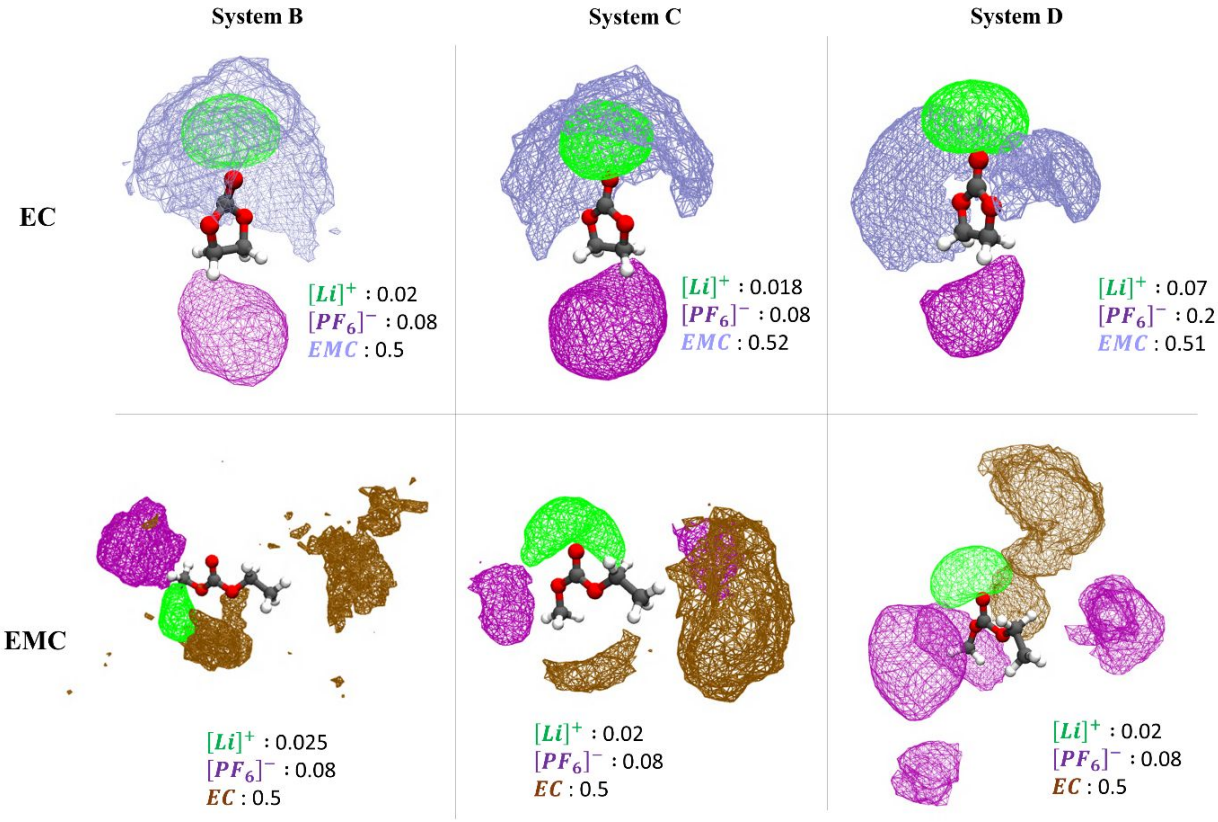

Figure 6. Volumetric probability density maps of PF_6^- (magenta clouds), Li^+ (green clouds) and the other solvent EMC/ EC (lavender clouds) with respect to EC and EMC molecules respectively for systems B, C and D. The probability density iso-values used to plot the volumetric maps are also depicted.

This results in a highly charge separated molecular ordering around EC. In contrast, for the EMC molecule, the volumetric density maps indicated a more distributed probability density for PF_6^- interaction which can be rationalized by the presence of positively charged ethyl and methyl groups on both sides of the EMC molecule. Amongst the ethyl and methyl groups, PF_6^- is observed to interact more with the methyl group. This is rationalized by the fact that the oxygen atom with ethyl group has a RESP derived partial charge of -0.62 while the oxygen atom attached to the methyl group has a partial charge of -0.43. PF_6^- being negatively charged is repelled to a greater extent by the ethyl group when compared to the methyl group due to the more negatively charged oxygen atom attached to the ethyl group. This is

manifested in the decreased volumetric probability of PF_6^- near ethyl group when compared to the methyl group.

Next, from a macroscopic context, we take a closer look at the solvation structure around the Li^+-ions in an attempt to identify factors that limit the value of transport properties and identify means to mitigate these limitations. We start with the macro-scale calculations of the diffusivities and conductivities presented above and conduct a sensitivity analysis of the various contributing species diffusivities (D_{ii} and D_{ij}). In the simplest case, this is accomplished by systematically increasing the component diffusivities one at a time, by a factor of 10 and observing the changes to the effective Fickian diffusivity and Li^+ conductivity. For instance, on System A, D_{ii} for Li^+ has a baseline value of 9.26e-11 m^2/s computed from MD calculations. The baseline Fickian diffusivity for this case is 3.61e-9 m^2/s and the Li^+ conductivity 2.54 mS/cm. Upon setting the D_{ii} value for Li^+ to ten times the baseline value, the values of these properties change to 9.37e-9 m^2/s and 9.19 mS/cm respectively. For this simple case, the increase in self-diffusivity corresponds to switching the charge carriers from Li^+ to a hypothetical ion with much lower atomic mass. This change in turn trickles through the cross-diffusion terms and eventually results in an improvement to the effective properties. Similar hypothetical changes to the D_{ii} and D_{ij} terms reveal that $D_{Li^+,EMC}$ values have the largest influence on improving transport at low $LiPF_6$ concentrations while improving self-diffusivity of EMC is most likely to be effective at higher salt concentrations. This is in line with some experimental observations: for instance Shim[60] showed that properties such as the bulk dielectric constant have limited influence on the solvation shell compared to local-concentrations of individual species. Other attempts to modify the EMC molecules include substituting the hydrogens in the molecule with alternate species. For example, Jow et al. propose the use of fluorinated EMC for improved transport properties. [65]

The presence of multiple stereo isotopes in the linear-chain carbonates has been used to reconcile differences between computed values for diffusivities and experimental measurements.[25] However, in our calculations (Figure 1) we found that the differences in binding energies between Li^+ and the carbonyl oxygens in the *cis* and *trans* configurations for EMC were less than 1 kcal/mol, which is within the bounds of accuracy of these methods. Alternately, binding of Li^+ to the oxygens in the ether position, in addition to the carbonyl groups has also been proposed, albeit at very small percentages. The self-diffusivity of the linear carbonate solvents can in turn be improved by opting for smaller chain lengths (e.g., replacing EMC with DMC). The marginal improvements to viscosities (0.65 cP for EMC versus 0.59 cP for DMC at 25^0C) however, are not adequate to bring about an increase in diffusivities that will help accomplish the fast-charge targets.

Typically, analysis of contributions from the EC molecules towards improving bulk transport properties are limited to higher dielectric constants and consequent increase in solubilities in addition to their excellent ability to form very stable SEI layers. This is because, interactions of EC molecules with Li^+ are limited to the carbonyl oxygen, which necessitates the rotation of the solvent molecule or a longer distance for the ion to traverse before accommodating additional interactions. However, in the context of fast charging, there are a few other properties worth examining closer:

i) The EC molecule, with a high dielectric constant dissociates the contact pair (Li^+–PF_6^-) and thus stabilizes Li^+ ions. In contrast, the linear carbonates reorient to solvate both dissociated Li^+ as well as the contact pairs. Bohn-Oppenheimer MD calculations by Borodin et al.[25] even suggest that the contact ion pairs may have a higher number of coordinated DMC molecules than for fully solvated Li^+ cations. This is one of the main drawbacks with improved solubilities realized from the use of small-chain linear solvent molecules: the transference numbers are still below target in these situations.

ii) Recent FTIR results reported by Liang and co-workers[66] showed that the formation and dissociation dynamics of Li^+-cyclic carbonate complexes are faster than those with the linear carbonate complexes. This aspect is crucial to accelerate solvation and mitigate plating of metallic lithium, as large fluxes of Li^+ tend to accumulate at the surface of the anode during extreme fast charge.

iii) Given the large difference in dielectric constants between cyclic and linear carbonates, EC-type molecules tend to form rigid solvation shells mitigating the "fluctuation" of solvents around the charge carriers during charge. [60]

Given these attributes, there are a few limitations to overcome, before considering cyclic molecules as effective solvents to improve fast charging capabilities. First off, the moment of inertia about the rotational axis of cyclic molecules is much bigger compared to the linear chain solvents. This in turn means that the carbonyl groups of the former set of compounds have to overcome a significantly higher energy barrier to rotate and interact with the Li^+ ions as discussed earlier. Secondly, the number of sites for Li^+ to bind are limited to the carbonyl groups in EC, thus exponentially decreasing the probability of solvation as the local salt concentration increases during fast charge. These limitations suggest alternate pathways to enhance Li^+ diffusion: the traditional carrier-based diffusion mechanism wherein the Li^+ is bound to a solvation shell will likely face constraints due to conflicting requirements of lower viscosities and higher solubilities under extreme fast charge conditions. However, a hopping-mechanism where the Li^+ jumps from one tailored site within a solvation shell to another is expected to result in faster diffusivities. [15,67,68] A similar argument is also supported by fast rotational dynamics in PF_6^- anions that are also bulky like the cyclic carbonates; but the presence of six conformal fluorine sites for the Li^+ to bind lowers the energy barrier significantly for rotation of these anions.[36] An equivalent configuration, where in there are multiple sites available for Li^+ to bind, without necessitating an increase in the mole-fraction of

the cyclic solvent molecules will likely accomplish the transport goals for Li^+ under extreme fast charging, without suffering from any further increase to viscosities under high salt concentrations.

In addition to these, design of a practical electrolyte system also entails a careful consideration of various additives used to alter properties in the bulk electrolyte as well as the interface. Detailed computation of electrolyte properties in the presence of multiple salts and/or additives have been extensively studied in the literature both experimentally [61] and computationally [32]. Alternate electrolyte formulations also consider modifying the anion: for example, Bis(fluorosulfonyl)imides or FSI- anions have been a contender in recent literature.[69] While the discussion presented in the current work is limited to the standard Gen-2 formulation as the benchmark, it is widely recognized that additives play an indispensable role in enhancing electrolyte properties, as do alternate salt formulations. Methods presented in the current work readily extend to analyzing enhancements to Li^+ transport in such systems.

4. Conclusions

Target values for extreme fast charging of lithium ion batteries set based on continuum level calculations are compared against predicted values obtained from molecular simulations. The Onsager-Stefan-Maxwell framework helps relate bulk transport properties to component-level interactions. MD simulations allow us to attribute limitations in diffusivity and conductivity to specific pair-wise interactions. There are still gaps in our understanding of ion-solvent interactions at very high local salt concentrations, which are beyond the scope of theoretical tools employed in this study. Careful choice of force fields and implementing appropriate solvent-phase simulations are key to understanding experimentally relevant interactions in concentrated electrolytes required for fast charging of lithium ion batteries. Detailed characterization of solvation shell composition and interactions between the charge carriers and solvent molecules as a function of salt concentrations reveal several options for rational design of electrolyte compositions tailored to extreme fast charge conditions. This approach also allows us to

understand limitations with commonly used solvents such as linear carbonates, that do not maintain transference numbers albeit exhibiting good diffusivities. This is due to the fact that the linear solvent molecules promote solvation of the ion-conducting salts as ion-pairs rather than solvating the Li^+ ions and are thus of limited practical value towards improving fast charge characteristics. Alternate approaches to design of solvent molecules, including functionalization of ethylene carbonate-based solvents to promote rapid solvation and improving robustness of the solvation shells, were identified. Many of these results agree very well with experimentally observed gaps in extreme fast charging. Results presented in here are a first step in designing composition of solvents accounting for both bulk-properties (such as viscosity) that are readily measured experimentally as well as local effects that are difficult to characterize. Based on these results specific recommendations to modify EC-type cyclic molecules and EMC-type linear molecules are currently being pursued to develop next generation electrolytes for extreme fast charging applications.

5. Acknowledgements

Funding for this work provided by the U.S. DOE Office of Vehicle Technology Extreme Fast Charge Program, Program manager Samuel Gillard is gratefully acknowledged. The research was performed using computational resources sponsored by the Department of Energy's Office of Energy Efficiency and Renewable Energy, located at the National Renewable Energy Laboratory. The U.S. Government retains and the publisher, by accepting the article for publication, acknowledges that the U.S. Government retains a nonexclusive, paid-up, irrevocable, worldwide license to publish or reproduce the published form of this work, or allow others to do so, for U.S. Government purposes.

6. References

[1] D. Howell, S. Boyd, B. Cunningham, S. Gillard, L. Slezak, S. Ahmed, I. Bloom, A. Burnham, K. Hardy, A.N. Jansen, P.A. Nelson, D.C. Robertson, T. Stephens, R. Vijayagopal, R.B. Carlson, F.

Dias, E.J. Dufek, C.J. Michelbacher, M. Mohanpurkar, D. Scoffield, M. Shirk, T. Tanim, M. Keyser, C. Kreuzer, O. Li, A. Markel, A. Meintz, A. Pesaran, S. Santhanagopalan, K. Smith, E. Wood, J. Zhang, Enabling Fast Charging: A Technology Gap Assessment, (2017).

[2] S. Ahmed, I. Bloom, A.N. Jansen, T. Tanim, E.J. Dufek, A. Pesaran, A. Burnham, R.B. Carlson, F. Dias, K. Hardy, M. Keyser, C. Kreuzer, A. Markel, A. Meintz, C. Michelbacher, M. Mohanpurkar, P.A. Nelson, D.C. Robertson, D. Scoffield, M. Shirk, T. Stephens, R. Vijayagopal, J. Zhang, Enabling fast charging – A battery technology gap assessment, J. Power Sources. 367 (2017) 250–262. https://doi.org/10.1016/j.jpowsour.2017.06.055.

[3] M. Keyser, A. Pesaran, Q. Li, S. Santhanagopalan, K. Smith, E. Wood, S. Ahmed, I. Bloom, E. Dufek, M. Shirk, A. Meintz, C. Kreuzer, C. Michelbacher, A. Burnham, T. Stephens, J. Francfort, B. Carlson, J. Zhang, R. Vijayagopal, K. Hardy, F. Dias, M. Mohanpurkar, D. Scoffield, A.N. Jansen, T. Tanim, A. Markel, Enabling fast charging – Battery thermal considerations, J. Power Sources. 367 (2017) 228–236. https://doi.org/10.1016/j.jpowsour.2017.07.009.

[4] A. Meintz, J. Zhang, R. Vijayagopal, C. Kreutzer, S. Ahmed, I. Bloom, A. Burnham, R.B. Carlson, F. Dias, E.J. Dufek, J. Francfort, K. Hardy, A.N. Jansen, M. Keyser, A. Markel, C. Michelbacher, M. Mohanpurkar, A. Pesaran, D. Scoffield, M. Shirk, T. Stephens, T. Tanim, Enabling fast charging – Vehicle considerations, J. Power Sources. 367 (2017) 216–227. https://doi.org/10.1016/j.jpowsour.2017.07.093.

[5] A. Burnham, E.J. Dufek, T. Stephens, J. Francfort, C. Michelbacher, R.B. Carlson, J. Zhang, R. Vijayagopal, F. Dias, M. Mohanpurkar, D. Scoffield, K. Hardy, M. Shirk, R. Hovsapian, S. Ahmed, I. Bloom, A.N. Jansen, M. Keyser, C. Kreuzer, A. Markel, A. Meintz, A. Pesaran, T.R. Tanim, Enabling fast charging – Infrastructure and economic considerations, J. Power Sources. 367 (2017) 237–249. https://doi.org/10.1016/j.jpowsour.2017.06.079.

[6] A.M. Colclasure, A.R. Dunlop, S.E. Trask, B.J. Polzin, A.N. Jansen, K. Smith, Requirements for Enabling Extreme Fast Charging of High Energy Density Li-Ion Cells while Avoiding Lithium Plating, J. Electrochem. Soc. 166 (2019) A1412–A1424. https://doi.org/10.1149/2.0451908jes.

[7] Y. Liu, Y. Zhu, Y. Cui, Challenges and opportunities towards fast-charging battery materials, Nat. Energy. 4 (2019) 540–550. https://doi.org/10.1038/s41560-019-0405-3.

[8] K. Xu, Electrolytes and interphases in Li-ion batteries and beyond, Chem. Rev. 114 (2014) 11503–11618. https://doi.org/10.1021/cr500003w.

[9] K. Xu, Nonaqueous liquid electrolytes for lithium-based rechargeable batteries, Chem. Rev. 104 (2004) 4303–4417. https://doi.org/10.1021/cr030203g.

[10] H.G. Buss, S.Y. Chan, N.A. Lynd, B.D. McCloskey, Nonaqueous Polyelectrolyte Solutions as Liquid Electrolytes with High Lithium Ion Transference Number and Conductivity, ACS Energy Lett. 2 (2017) 481–487. https://doi.org/10.1021/acsenergylett.6b00724.

[11] E.R. Logan, D.S. Hall, M.M.E. Cormier, T. Taskovic, M. Bauer, I. Hamam, H. Hebecker, L. Molino, J.R. Dahn, Ester-Based Electrolytes for Fast Charging of Energy Dense Lithium-Ion Batteries, J. Phys. Chem. C. 124 (2020) 12269–12280. https://doi.org/10.1021/acs.jpcc.0c02370.

[12] J. Li, H. Li, X. Ma, W. Stone, S. Glazier, E. Logan, E.M. Tonita, K.L. Gering, J.R. Dahn, Methyl Acetate as a Co-Solvent in NMC532/Graphite Cells, J. Electrochem. Soc. 165 (2018) A1027–A1037. https://doi.org/10.1149/2.0861805jes.

[13] D.M. Seo, O. Borodin, S.-D. Han, Q. Ly, P.D. Boyle, W.A. Henderson, Electrolyte Solvation and Ionic Association. I. Acetonitrile-Lithium Salt Mixtures: Intermediate and Highly Associated Salts, J. Electrochem. Soc. 159 (2012) A553–A565. https://doi.org/10.1149/2.jes112264.

[14] D.M. Seo, O. Borodin, S.-D. Han, P.D. Boyle, W.A. Henderson, Electrolyte Solvation and Ionic Association. II. Acetonitrile-Lithium Salt Mixtures: Highly Dissociated Salts, J. Electrochem. Soc.

159 (2012) A1489–A1500. https://doi.org/10.1149/2.035209jes.

[15] D.M. Seo, O. Borodin, D. Balogh, M. O'Connell, Q. Ly, S.-D. Han, S. Passerini, W.A. Henderson, Electrolyte Solvation and Ionic Association III. Acetonitrile-Lithium Salt Mixtures–Transport Properties, J. Electrochem. Soc. 160 (2013) A1061–A1070. https://doi.org/10.1149/2.018308jes.

[16] S.-D. Han, O. Borodin, J.L. Allen, D.M. Seo, D.W. McOwen, S.-H. Yun, W.A. Henderson, Electrolyte Solvation and Ionic Association. IV. Acetonitrile-Lithium Difluoro(oxalato)borate (LiDFOB) Mixtures, J. Electrochem. Soc. 160 (2013) A2100–A2110. https://doi.org/10.1149/2.094309jes.

[17] S.-D. Han, O. Borodin, D.M. Seo, Z.-B. Zhou, W.A. Henderson, Electrolyte Solvation and Ionic Association. V. Acetonitrile-Lithium Bis(fluorosulfonyl)imide (LiFSI) Mixtures, J. Electrochem. Soc. 161 (2014) A2042–A2053. https://doi.org/10.1149/2.0101414jes.

[18] O. Borodin, S.-D. Han, J.S. Daubert, D.M. Seo, S.-H. Yun, W.A. Henderson, Electrolyte Solvation and Ionic Association. VI. Acetonitrile-Lithium Salt Mixtures: Highly Associated Salts Revisited, J. Electrochem. Soc. 162 (2015) A501–A510. https://doi.org/10.1149/2.0891503jes.

[19] W.A. Henderson, D.M. Seo, S.-D. Han, O. Borodin, Electrolyte Solvation and Ionic Association. VII. Correlating Raman Spectroscopic Data with Solvate Species, J. Electrochem. Soc. 167 (2020) 110551. https://doi.org/10.1149/1945-7111/aba44a.

[20] Y. Yamada, K. Furukawa, K. Sodeyama, K. Kikuchi, M. Yaegashi, Y. Tateyama, A. Yamada, Unusual stability of acetonitrile-based superconcentrated electrolytes for fast-charging lithium-ion batteries, J. Am. Chem. Soc. 136 (2014) 5039–5046. https://doi.org/10.1021/ja412807w.

[21] V. Nilsson, Highly Concentrated Electrolytes for Rechargeable Lithium Batteries, Chalmers University of Technology, 2020.

[22] E.R. Logan, J.R. Dahn, Electrolyte Design for Fast-Charging Li-Ion Batteries, Trends Chem. 2 (2020) 354–366. https://doi.org/10.1016/j.trechm.2020.01.011.

[23] M.C. Smart, B. V. Ratnakumar, L.D. Whitcanack, K.B. Chin, S. Surampudi, H. Croft, D. Tice, R. Staniewicz, Improved low-temperature performance of lithium-ion cells with quaternary carbonate-based electrolytes, J. Power Sources. 119–121 (2003) 349–358. https://doi.org/10.1016/S0378-7753(03)00154-X.

[24] C.C. Su, M. He, R. Amine, T. Rojas, L. Cheng, A.T. Ngo, K. Amine, Solvating power series of electrolyte solvents for lithium batteries, Energy Environ. Sci. 12 (2019) 1249–1254. https://doi.org/10.1039/c9ee00141g.

[25] O. Borodin, M. Olguin, P. Ganesh, P.R.C. Kent, J.L. Allen, W.A. Henderson, Competitive lithium solvation of linear and cyclic carbonates from quantum chemistry, Phys. Chem. Chem. Phys. 18 (2016) 164–175. https://doi.org/10.1039/c5cp05121e.

[26] L.O. Valøen, J.N. Reimers, Transport Properties of LiPF6 -Based Li-Ion Battery Electrolytes, J. Electrochem. Soc. 152 (2005) A882. https://doi.org/10.1149/1.1872737.

[27] S. Stewart, J. Newman, Measuring the Salt Activity Coefficient in Lithium-Battery Electrolytes, J. Electrochem. Soc. 155 (2008) A458. https://doi.org/10.1149/1.2904526.

[28] C.M. Tenney, R.T. Cygan, Analysis of molecular clusters in simulations of lithium-ion battery electrolytes, J. Phys. Chem. C. 117 (2013) 24673–24684. https://doi.org/10.1021/jp4039122.

[29] A. Muralidharan, M.I. Chaudhari, L.R. Pratt, S.B. Rempe, Molecular Dynamics of Lithium Ion Transport in a Model Solid Electrolyte Interphase, Sci. Rep. 8 (2018) 1–8. https://doi.org/10.1038/s41598-018-28869-x.

[30] A. Dave, K.L. Gering, J.M. Mitchell, J. Whitacre, V. Viswanathan, Benchmarking Conductivity Predictions of the Advanced Electrolyte Model (AEM) for Aqueous Systems, J. Electrochem. Soc.

167 (2020) 013514. https://doi.org/10.1149/2.0142001jes.

[31] M.J. Hossain, G. Pawar, B. Liaw, K.L. Gering, E.J. Dufek, A.C.T. van Duin, Lithium-electrolyte solvation and reaction in the electrolyte of a lithium ion battery: A ReaxFF reactive force field study, J. Chem. Phys. 152 (2020) 184301. https://doi.org/10.1063/5.0003333.

[32] E.R. Logan, K.L. Gering, X. Ma, J.R. Dahn, Electrolyte Development for High-Performance Li-Ion Cells: Additives, Solvents, and Agreement with a Generalized Molecular Model, Electrochem. Soc. Interface 28 (2019) 49.

[33] O. Borodin, G.D. Smith, Quantum chemistry and molecular dynamics simulation study of dimethyl carbonate: Ethylene carbonate electrolytes doped with LiPF6, J. Phys. Chem. B. 113 (2009) 1763–1776. https://doi.org/10.1021/jp809614h.

[34] B. Ravikumar, M. Mynam, B. Rai, Effect of Salt Concentration on Properties of Lithium Ion Battery Electrolytes: A Molecular Dynamics Study, J. Phys. Chem. C. 122 (2018) 8173–8181. https://doi.org/10.1021/acs.jpcc.8b02072.

[35] K. Xu, Y. Lam, S.S. Zhang, T.R. Jow, T.B. Curtis, Solvation sheath of Li+ in nonaqueous electrolytes and its implication of graphite/electrolyte interface chemistry, J. Phys. Chem. C. 111 (2007) 7411–7421. https://doi.org/10.1021/jp068691u.

[36] S. Han, Structure and dynamics in the lithium solvation shell of nonaqueous electrolytes, Sci. Rep. 9 (2019) 1–10. https://doi.org/10.1038/s41598-019-42050-y.

[37] N. Kumar, J.M. Seminario, Lithium-ion model behavior in an ethylene carbonate electrolyte using molecular dynamics, J. Phys. Chem. C. 120 (2016) 16322–16332. https://doi.org/10.1021/acs.jpcc.6b03709.

[38] D. Bedrov, J.P. Piquemal, O. Borodin, A.D. MacKerell, B. Roux, C. Schröder, Molecular Dynamics Simulations of Ionic Liquids and Electrolytes Using Polarizable Force Fields, Chem. Rev.

119 (2019) 7940–7995. https://doi.org/10.1021/acs.chemrev.8b00763.

[39] A.D. Becke, Density-functional thermochemistry. III. The role of exact exchange, J. Chem. Phys. 98 (1993) 5648–5652. https://doi.org/10.1063/1.464913.

[40] C. Lee, W. Yang, R.G. Parr, Development of the Colle-Salvetti correlation-energy formula into a functional of the electron density, Phys. Rev. B. 37 (1988) 36–39.

[41] Frisch; M. J.; Trucks; G. W.; Schlegel; H. B.; Scuseria; G. E.; Robb; M. A.; Cheeseman; J. R.; Scalmani; G.; Barone; V.; Petersson; G. A.; Nakatsuji; H.; Li; X.; Caricato; M.; Marenich; A. V.; Bloino; J.; Janesko; B. G.; Gomperts; R.; Mennucci; B.; Hratch, (2016).

[42] Y. Zhang, Y. Zhang, M.J. McCready, E.J. Maginn, Evaluation and Refinement of the General AMBER Force Field for Nineteen Pure Organic Electrolyte Solvents, J. Chem. Eng. Data. 63 (2018) 3488–3502. https://doi.org/10.1021/acs.jced.8b00382.

[43] C.I. Bayly, P. Cieplak, W.D. Cornell, P.A. Kollman, A well-behaved electrostatic potential based method using charge restraints for deriving atomic charges: The RESP model, J. Phys. Chem. 97 (1993) 10269–10280. https://doi.org/10.1021/j100142a004.

[44] J. Wang, W. Wang, P.A. Kollman, D.A. Case, Automatic atom type and bond type perception in molecular mechanical calculations, J. Mol. Graph. Model. 25 (2006) 247–260. https://doi.org/10.1016/j.jmgm.2005.12.005.

[45] J. Wang, R.M. Wolf, J.W. Caldwell, P.A. Kollman, D.A. Case, Development and testing of a general Amber force field, J. Comput. Chem. 25 (2004) 1157–1174. https://doi.org/10.1002/jcc.20035.

[46] A. Chaumont, G. Wipff, Solvation of M3+ lanthanide cations in room-temperature ionic liquids. A molecular dynamics investigation, Phys. Chem. Chem. Phys. 5 (2003) 3481–3488. https://doi.org/10.1039/b305091b.

[47] I.S. Joung, T.E. Cheatham, Determination of alkali and halide monovalent ion parameters for use in explicitly solvated biomolecular simulations, J. Phys. Chem. B. 112 (2008) 9020–9041. https://doi.org/10.1021/jp8001614.

[48] V.S. Bharadwaj, T.C. Schutt, T.C. Ashurst, C.M. Maupin, Elucidating the conformational energetics of glucose and cellobiose in ionic liquids, Phys. Chem. Chem. Phys. 17 (2015) 10668–10678. https://doi.org/10.1039/c5cp00118h.

[49] G.A. Hegde, V.S. Bharadwaj, C.L. Kinsinger, T.C. Schutt, N.R. Pisierra, C.M. Maupin, Impact of water dilution and cation tail length on ionic liquid characteristics: Interplay between polar and non-polar interactions, J. Chem. Phys. 145 (2016). https://doi.org/10.1063/1.4960511.

[50] T.C. Schutt, V.S. Bharadwaj, G.A. Hegde, A.J. Johns, C. Mark Maupin, In silico insights into the solvation characteristics of the ionic liquid 1-methyltriethoxy-3-ethylimidazolium acetate for cellulosic biomass, Phys. Chem. Chem. Phys. 18 (2016) 23715–23726. https://doi.org/10.1039/c6cp03235d.

[51] V.S. Bharadwaj, N.M. Eagan, N.M. Wang, M.W. Liberatore, C.M. Maupin, Molecular Simulations of Fatty-Acid Methyl Esters and Representative Biodiesel Mixtures, ChemPhysChem. 16 (2015) 2810–2817. https://doi.org/10.1002/cphc.201500453.

[52] M.R. Shirts, C. Klein, J.M. Swails, J. Yin, M.K. Gilson, D.L. Mobley, D.A. Case, E.D. Zhong, Lessons learned from comparing molecular dynamics engines on the SAMPL5 dataset, J. Comput. Aided. Mol. Des. 31 (2017) 147–161. https://doi.org/10.1007/s10822-016-9977-1.

[53] L. Martinez, R. Andrade, E.G. Birgin, J.M. Martínez, PACKMOL: A package for building initial configurations for molecular dynamics simulations, J. Comput. Chem. 30 (2009) 2157–2164. https://doi.org/10.1002/jcc.21224.

[54] R.. Hockney, J.. Eastwood, Computer Simulation Using Particles, CRC Press, 1988.

[55] M.T. Humbert, Y. Zhang, E.J. Maginn, PyLAT: Python LAMMPS Analysis Tools, J. Chem. Inf. Model. 59 (2019) 1301–1305. https://doi.org/10.1021/acs.jcim.9b00066.

[56] W. Humphrey, A. Dalke, K. Schulten, VMD: Visual Molecular Dynamics, J. Mol. Graph. 14 (1996) 33–38. https://doi.org/10.1016/0263-7855(96)00018-5.

[57] M.J. Frisch, G.W. Trucks, H.B. Schlegel, G.E. Scuseria, M.A. Robb, J.R. Cheeseman, G. Scalmani, V. Barone, G.A. Petersson, H. Nakatsuji, X. Li, M. Caricato, A. V Marenich, J. Bloino, B.G. Janesko, R. Gomperts, B. Mennucci, H.P. Hratchian, J. V Ortiz, A.F. Izmaylov, J.L. Sonnenberg, Williams, F. Ding, F. Lipparini, F. Egidi, J. Goings, B. Peng, A. Petrone, T. Henderson, D. Ranasinghe, V.G. Zakrzewski, J. Gao, N. Rega, G. Zheng, W. Liang, M. Hada, M. Ehara, K. Toyota, R. Fukuda, J. Hasegawa, M. Ishida, T. Nakajima, Y. Honda, O. Kitao, H. Nakai, T. Vreven, K. Throssell, J.A. Montgomery Jr., J.E. Peralta, F. Ogliaro, M.J. Bearpark, J.J. Heyd, E.N. Brothers, K.N. Kudin, V.N. Staroverov, T.A. Keith, R. Kobayashi, J. Normand, K. Raghavachari, A.P. Rendell, J.C. Burant, S.S. Iyengar, J. Tomasi, M. Cossi, J.M. Millam, M. Klene, C. Adamo, R. Cammi, J.W. Ochterski, R.L. Martin, K. Morokuma, O. Farkas, J.B. Foresman, D.J. Fox, Gaussian 16 Rev. C.01, (2016).

[58] Y. Zhao, D.G. Truhlar, The M06 suite of density functionals for main group thermochemistry, thermochemical kinetics, noncovalent interactions, excited states, and transition elements: two new functionals and systematic testing of four M06-class functionals and 12 other function, Theor. Chem. Acc. 120 (2008) 215–241. https://doi.org/10.1007/s00214-007-0310-x.

[59] J.A.M. Jr., M.J. Frisch, J.W. Ochterski, G.A. Petersson, A complete basis set model chemistry. VI. Use of density functional geometries and frequencies, J. Chem. Phys. 110 (1999) 2822–2827. https://doi.org/10.1063/1.477924.

[60] Y. Shim, Computer simulation study of the solvation of lithium ions in ternary mixed carbonate

electrolytes: Free energetics, dynamics, and ion transport, Phys. Chem. Chem. Phys. 20 (2018) 28649–28657. https://doi.org/10.1039/c8cp05190a.

[61] D.S. Hall, M. Nie, L. D. Ellis, S.L. Glazier, S. Hyatt, R. Petibon, A. Xiao, W.M. Lamanna, K. Smith, I.G. Hill, J.R. Dahn, Surface-Electrolyte Interphase Formation in Lithium-Ion Cells Containing Pyridine Adduct Additives, J. Electrochem. Soc. 163 (2016) A773–A780. https://doi.org/10.1149/2.1091605jes.

[62] S.U. Kim, V. Srinivasan, A Method for Estimating Transport Properties of Concentrated Electrolytes from Self-Diffusion Data, J. Electrochem. Soc. 163 (2016) A2977–A2980. https://doi.org/10.1149/2.0541614jes.

[63] R. Taylor, R. Krishna, Multicomponent mass transfer, 1961. https://doi.org/10.1002/aic.690070407.

[64] John Newman, K.E. Thomas-Alyea, Electrochemical Systems, Wiley-IEEE, 2004. file:///C:/Users/youhe/Downloads/kdoc_o_00042_01.pdf.

[65] T.R. Jow, K. Xu, O. Borodin, M. Ue, Electrolytes for Lithium and Lithium-Ion Batteries, Springer, 2014. https://www.springer.com/gp/book/9781493903016.

[66] C. Liang, K. Kwak, M. Cho, Revealing the Solvation Structure and Dynamics of Carbonate Electrolytes in Lithium-Ion Batteries by Two-Dimensional Infrared Spectrum Modeling, J. Phys. Chem. Lett. 8 (2017) 5779–5784. https://doi.org/10.1021/acs.jpclett.7b02623.

[67] P. Ganesh, D.E. Jiang, P.R.C. Kent, Accurate static and dynamic properties of liquid electrolytes for Li-ion batteries from ab initio molecular dynamics, J. Phys. Chem. B. 115 (2011) 3085–3090. https://doi.org/10.1021/jp2003529.

[68] O. Borodin, G. V. Zhuang, P.N. Ross, K. Xu, Molecular dynamics simulations and experimental study of lithium ion transport in dilithium ethylene dicarbonate, J. Phys. Chem. C. 117 (2013) 7433–

7444. https://doi.org/10.1021/jp4000494.

[69] Z. Du, D.L. Wood III, I. Belharouak, Electrochem. Communications, 103 (2019) 109-113. https://doi.org/10.1016/j.elecom.2019.04.013